4th URSI AT-RASC, Gran Canaria, 19-24 May 2024

Highly Compact Microfluidically Frequency-Tunable Self-Duplexing Antenna for Sub 6-GHz 5G Applications

Rusan Kumar Barik*(1, 2), Xiaoguang Liu(1), and Slawomir Koziel(2, 3)
(1) School of Microelectronics, Southern University of Science and Technology, Shenzhen, China
(2) Engineering Optimization and Modeling Center, Reykjavik University, 102 Reykjavik, Iceland
(3) Faculty of Electronics, Telecommunications and Informatics, Gdansk University of Technology, 80-233 Gdansk, Poland

Abstract

This paper proposes a microfluidic frequency tunable half-mode substrate-integrated waveguide (HMSIW) self-duplexing antenna for 5G applications. An inverted T-shaped slot is introduced on the top conducting plane of the HMSIW to create two unequal radiating patches. These are fed using 50Ω microstrip lines to operate at two distinct frequency bands with inherent self-duplexing properties. An equivalent circuit is established to describe the working principle of the antenna. Subsequently, three empty cylindrical vias corresponding to each radiating patch are created on the bottom plane. The vias are poured with different dielectric fluids to enable frequency tunability. Finally, a prototype of the suggested antenna is manufactured and experimentally validated. The manufactured antenna offers wide tuning ranges from 3.2 GHz to 3.66 GHz and 4.5 GHz to 5.07 GHz at the first and the second resonating bands, respectively. Additionally, the prototype shows good efficiency, appropriate gain, isolation, and a lower footprint than similar state-of-the-art devices documented in the literature.

1. Introduction

Modern wireless systems demand compact, multi-functional, and reconfigurable radio frequency front-end components. The concept of self-diplexing antennas has garnered significant attention since it eliminates the need for an extra diplexer circuit, resulting in a reduction in complexity, cost, and footprint area [1]. Realization of substrate-integrated waveguide-based self-diplexing antennas (SDAs) has recently attracted a lot of attention because of its many desirable properties, including small size, planar architecture, ease of fabrication, and excellent radiation characteristics [2-4]. Several frequency tunable self-duplexing antennas have been designed based on varactor diodes [5-7]. These antennas have limited power handling capability and require a biasing circuit, which raises the circuit's complexity, size, and cost.
On the other hand, a microfluidically-based reconfigurable technique offers an excellent alternative solution for the design of microwave components with enables high power handling capability and linearity [8-10]. In [8], a monopole antenna has been implemented for frequency tunability based on the microfluidic technique. In [9], a wideband monopole antenna has been realized with frequency tunable using liquid metal. A microfluidically frequency-reconfigurable self-diplexing antenna has been presented in [10], albeit with large footprint and smaller tuning range.

In this paper, a highly compact self-diplexing frequency tunable antenna based on a microfluidic technique has been presented. A detailed design procedure, parametric analysis, and development of an equivalent circuit have been discussed. A prototype has been manufactured and experimentally verified. The proposed antenna has a smaller footprint area of $0.093\lambda_g^2$ with the frequency-tuning ranges of 14.37% and 12.37%.

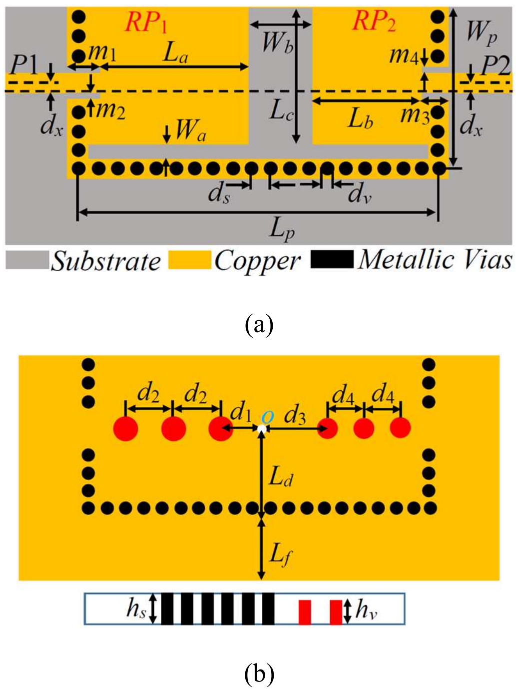

Figure 1. Schematic of the proposed frequency tunable self-duplexing antenna. (a) front-view. (b) back-view. The final optimized dimensions are: L_p = 27, W_p = 14.6, L_a = 9.52, W_a = 1.0, L_b = 7.265, W_b = 4.405, L_c = 12.8, L_d = 7.8, L_f = 5.0, m_1 = 4.03, m_2 = 0.52, m_3 = 2.63, m_4 = 0.51, d_1 = 2.5, d_2 = 3.0, d_3 = 5.5, d_4 = 2.5, d_s = 1.0, d_v = 1.8, h_s = 0.762, h_v = 0.562.

2. Frequency Tunable Self-Diplexing Antenna

2.1 Antenna Configuration and Analysis

Fig. 1 shows the schematic of the proposed frequency tunable self-diplexing antenna (FTSDA) with optimized dimensions. The proposed structure constructed by using a half-mode SIW cavity, two 50Ω microstrip feeding lines, and an inverted T-shaped slot (TSS). The step-by-step design approach is depicted in Fig. 2. Step-1 realizes a conventional full-mode SIW cavity of 29.2 × 27 mm^2 to operate at TE_{110} mode (4.63 GHz). In Step-2, the full-mode SIW is divided horizontally into two resonators named as half-mode (HM) cavity, by doing so the size is reduced by 50%. The resonating frequency of the suggested half-mode resonator (HMR) is computed by applying [3]:

$$f_{mn0}^{HMR} = \frac{1}{2\sqrt{\mu\varepsilon}}\sqrt{\left(\frac{m\pi}{L_{eff}^{HMR}}\right)^2 + \left(\frac{n\pi}{2W_{eff}^{HMR}}\right)^2} \quad (1)$$

$$\begin{cases} L_{eff}^{HMR} = L_p - 1.08\dfrac{d_v^{\,2}}{d_s} + 0.1\dfrac{d_v^{\,2}}{L_p} \\ W_{eff}^{HMR} = W_p - 1.08\dfrac{d_v^{\,2}}{d_s} + 0.1\dfrac{d_v^{\,2}}{W_p} \end{cases} \quad (2)$$

where L_{eff} and W_{eff} are the effective length and width of the HMR. The diameter d_v and the center-to-center spacing d_s of metallic vias are chosen by the relationship of $d_v/\lambda \leq 0.1$ and $d_v/d_s \geq 2$, to mitigate the energy loss via metallic vias. The eigen-mode solver is employed to both resonators and the computed electric-fields are depicted in Fig. 3. In Step-3, two 50Ω microstrip feeding lines are attached to the HM resonator. Subsequently, two radiating patches (RP1 and RP2) are made by arranging an inverted TSS on top of the HM resonator. This arrangement results in two radiating frequency with self-diplexing properties. In order to attain a good matching, inline feeding is employed as shown in Step-4 (Top). To understand the radiation technique, the surface current distributions related to the ports are estimated, as Fig. 4 illustrates. Looking to Fig. 4(a), it is observed that the maximum current is found near Port 1 whereas no significant current flown at Port 2. Similarly, as can be seen in Fig. 4(b), maximum current is observed near Port 2 while no current flows through Port 1. Thus, a self-diplexing operation is established.

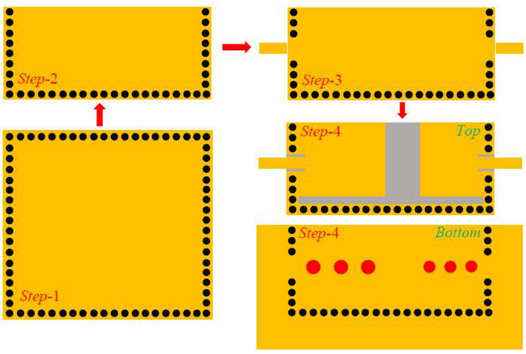

Figure 2. A step-by-step design process.

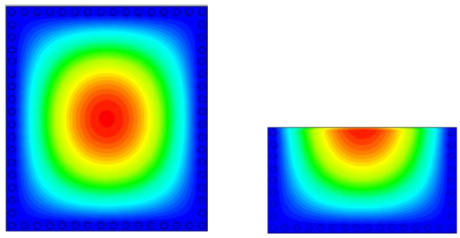

(a) (b)

Figure 3. Electric-field distributions of the conventional (a) full-mode and (b) half-mode resonators.

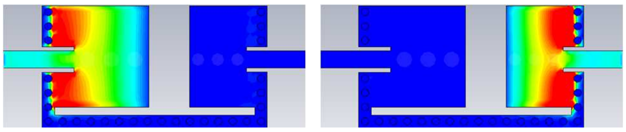

(a) (b)

Figure 4. Surface current distributions of the suggested FTSDA with excitations at (a) Port 1 and (b) Port 2.

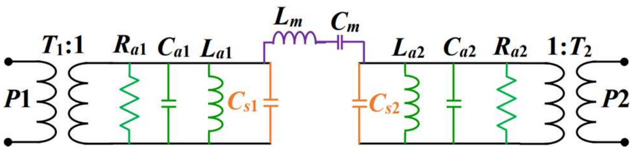

Figure 5. Equivalent circuit of the suggested FTSDA. The electrical parameters are: R_{a1} = 378Ω, C_{a1} = 0.107 pF, L_{a1} = 0.4654 nH, C_{s1} = 4.1996 pF, R_{a1} = 190Ω, C_{a1} = 0.053 pF, L_{a1} = 0.145 nH, C_{s1} = 6.974 pF, T_1 = 0.365, T_2 = 0.499.

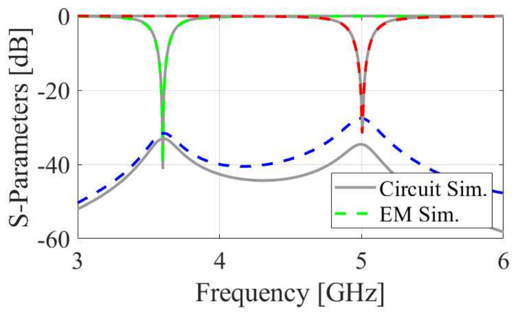

Figure 6. Equivalent circuit and full-wave simulated S-parameters of the suggested FTSDA.

2.2 Equivalent Circuit

To comprehend the size reduction and operation of the proposed FTSDA, an analogous circuit model is created. Fig. 5 shows an equivalent circuit of the suggested FTSDA. Each radiating patch is modelled as shunt connected resistance, inductance, and capacitance. RP_1 is represented by shunt connected R_{a1}, C_{a1}, and L_{a1} whereas RP_2 is expressed as shunt connected R_{a2}, C_{a2}, and L_{a2}. The extra capacitances C_{s1} and C_{s2} are produced due to the slots associated with RP_1 and RP_2, respectively. Theses capacitances create capacitive loading which is responsible for size reduction. The mutual coupling between the ports are represented by the series connected L_m and C_m. The transformers T_1 and T_2 are utilized for impedance matching at Port 1 and Port 2, respectively.

2.3 Frequency Reconfigurability

One of the main features of the proposed SDA is frequency reconfigurability using microfluidic channels. Three empty vias are created on each radiating patches, which are poured with different dielectric fluids to enable reconfigurability. In this work, the empty vias are poured with air, acetone (ε_r = 6.02), ethyl acetate (ε_r = 20.2), and distilled water (ε_r = 78.4) to alter the frequency bands. Fig. 7 shows the frequency tunability at individual ports when all the empty vias are filled with the dielectric liquids. When the channels associated with Port 1 is filled with dielectric fluids, the frequency is tuned from 3.2 GHz to 3.66 GHz (a tuning range of 14.27-percent). A frequency tuning range of 12.67-percent (from 4.5 GHz to 5.07 GHz) is obtained by filling the channels associated with Port 2. This frequency range is suitable for sub-6 GHz 5G applications.

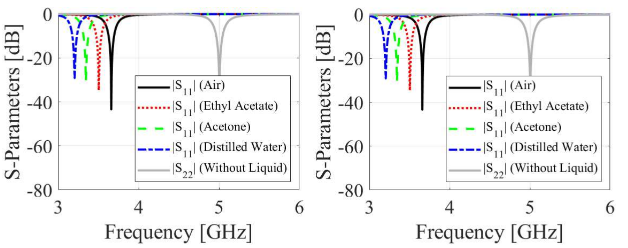

(a) (b)

Figure 7. EM simulation and equivalent circuit simulation S-parameters of the suggested FTSDA.

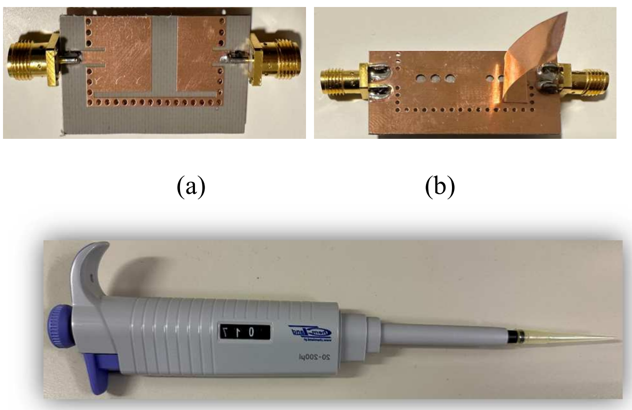

(a) (b)

(c)

Figure 8. Photograph of the manufactured FTSDA (a) front-view, (b) back-view and (c) injector/rectractor.

3. Fabrication and Measurement

Figures 8(a) and (b) show the photograph of the manufactured frequency-tunable SDA. The prototype is constructed on a Rogers AD250 substrate with a permittivity of 2.5, thickness of 0.762-mm, and tangential loss of 0.0014. The footprint of the fabricated SDA is $0.093\lambda_g^2$. The measurements are recorded by pouring the fluidic vias with air or distilled water as shown in Fig. 8(b). The injection and retraction are carried out by using a single channel pipet as depicted in Fig. 8(c). After pouring the fluids into the empty vias, a copper tape is used to cover them to retain the ground plane properties. A Rohde and Schwarz vector network analyzer is utilized to record the S-parameters. The radiation patterns and realized gain are obtained by employing an automatic anechoic chamber. Every measurement is performed by applying excitation at Port 1, while a 50-ohm load impedance is used to terminate Port 2, and vice versa.

Fig. 9 shows the EM simulation and tested S-parameters of the manufactured FTSDA for distilled water-poured vias. The predicted reflection coefficients –29.2 dB and –22.1 whereas the tested ones are –20.75 dB and –19.2 dB at 3.2 GHz and 4.5 GHz, respectively. The measured (predicted) isolations are 32.5 dB (31.1dB) and 37.3 dB (28.47 dB) at 3.2 GHz and 4.5 GHz, respectively. A frequency tuning range of 14.37% (460 MHz) and 12.67% (570 MHz) at first and second frequency bands.

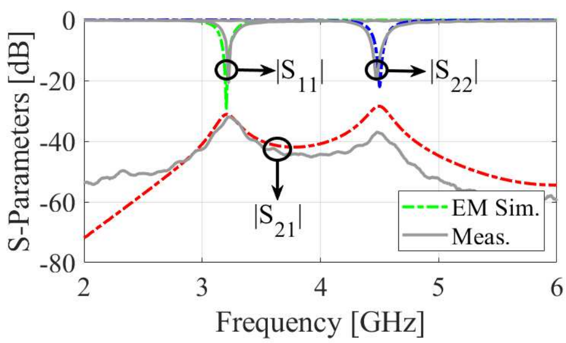

Figure 9. S-parameters of the FTSDA for distilled water-poured vias.

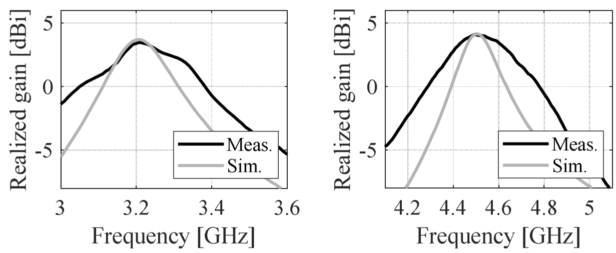

(a) (b)

Figure 10. Realized gains of the FTSDA for distilled water-poured vias. (a) At 3.2 GHz and (b) at 4.5 GHz.

Fig. 10 shows the EM simulation and tested realized gains of the suggested antenna for distilled water-poured vias. The predicted (measured) realized gains are recorded at 3.2 GHz and 4.5 GHz as 3.69 dBi (3.2 dBi) and 4.16 dBi (3.87 dBi), respectively. Fig. 11 shows the normalized far-field patterns of the fabricated SDA at ϕ = 0° (E-plane) and ϕ = 90° (H-plane) for both ports excitation. The cross-polarization level is below –20 dB and the front-to-back ratio is greater than 15 dB, as can be shown in Figure 11. A small discrepancy is seen between predicted and measured results due to the fabrication tolerance, connector loss, and precision of the substrate. Table 1 shows the measured performances in terms of tuning range, realized gain, and isolation of the fabricated SDA. The suggested FTSDA offers smallest footprint, broad frequency reconfigurability, good S-parameters, and far-field characteristics, which makes the FTSDA more suitable for sub-6GHz 5G applications.

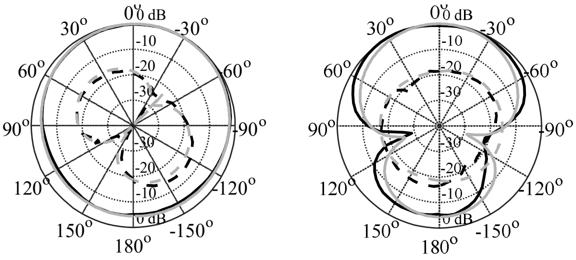

(a)

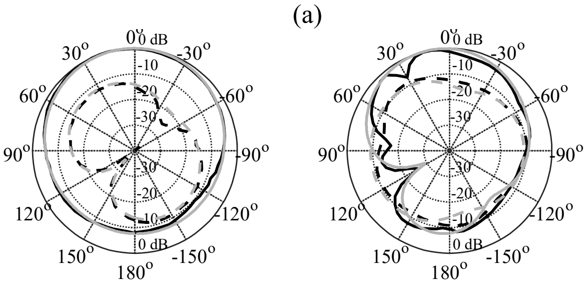

(b)

Figure 11. Normalized radiation patterns of the manufactured FTSDA for distilled water-poured vias: (a) 3.2 GHz and (b) 4.5 GHz. [Simulation – grey, experiment – black); H-plane (left), E-plane (right); copol – solid, crosspol – dashed].

Table 1
Measured Performances of SDFTA

Port Excitation	Tunable Freq. (GHz)	Isolation (dB)	Realized Gain (dBi)
Port 1	3.2 – 3.66	31.15 – 31.68	3.69 – 4.09
Port 2	4.5 – 5.07	27.45 – 28.47	4.15 – 4.19

4 Conclusion

In this paper, a compact frequency reconfigurable self-diplexing antenna based on microfluidic channels has been presented for 5G applications. The proposed antenna has been constructed by utilizing a half-mode SIW cavity. Three empty vias are created within the bottom plane associated with individual patches, which are poured with dielectric fluids to facilitate frequency reconfigurability. A detailed structural development, equivalent circuit model, and frequency reconfigurability have been discussed. Finally, a prototype has been fabricated and experimentally demonstrated. The fabricated antenna offers tuning ranges of 460 MHz and 570 MHz with a smaller footprint area of $0.093\lambda_g^2$. The tested reflection coefficients, isolation, and realized gains are greater than –20 dB, 27.45 dB, and 3.74 dBi, respectively.

5. Acknowledgements

This work was supported in part by the Icelandic Centre for Research (RANNIS) Grant 217771 and in part by the National Science Centre of Poland Grant 2020/37/B/ST7/01448.

References

[1] Y. C. Lu and Y. C. Lin, “A mode-based design method for dual-band and self-diplexing antennas using double T-stubs loaded aperture,” *IEEE Trans. Ant. Propag.*, **60**, 12, Dec. 2012, pp. 5596-5603, doi: 10.1109/TAP.2012.2211852.

[2] R. K. Barik, S. Koziel, Q. S. Cheng and S. Szczepanski, “Highly miniaturized self-diplexed U-shaped slot antenna based on shielded QMSIW,” *IEEE Access*, **9**, Nov. 2021, pp. 158926-158935, doi: 10.1109/ACCESS.2021.3131174.

[3] R. K. Barik, Q. S. Cheng, S. K. K. Dash, N. C. Pradhan, and K. S. Subramanian, “Design of a compact orthogonal fed self-diplexing bowtie-ring slot antenna based on substrate integrated waveguide,” *Int J RF Microw Comput Aided Eng.*, **30**, 11, Nov. 2020, pp. e22422, doi: 10.1002/mmce.22422.

[4] H. Kang and S. Lim, “Electrically small dual-band reconfigurable complementary split-ring resonator (CSRR)-loaded eighth-mode substrate integrated waveguide (EMSIW) antenna,” *IEEE Trans. Ant. Propag.*, **62**, 5, May 2014, pp. 2368-2373, doi: 10.1109/TAP.2014.2308532.

[5] A. Boukarkar, X. Q. Lin, Y. Jiang and Y. Q. Yu, “A tunable dual-fed self-diplexing patch antenna,” *IEEE Trans. Ant. Propag.*, **65**, 6, June 2017, pp. 2874-2879, doi: 10.1109/TAP.2017.2689035.

[6] S. -A. Malakooti and C. Fumeaux, “Frequency-agile self-diplexing antenna,” 4th Australian Microwave Symposium (AMS), Sydney, NSW, Australia, 2020, pp. 1-2, doi: 10.1109/AMS48904.2020.9059452.

[7] A. Iqbal, J. J. Tiang, C. K. Lee and N. K. Mallat, “SIW cavity backed self-diplexing tunable antenna,” *IEEE Trans. Ant. Propag.*, **69**, 8, Aug. 2021, pp. 5021-5025, doi: 10.1109/TAP.2021.3060024.

[8] A. Dey and G. Mumcu, “Microfluidically controlled frequency-tunable monopole antenna for high-power applications,” *IEEE Ant. Wireless Propag. Lett.*, **15**, June 2015, pp. 226-229, doi: 10.1109/LAWP.2015.2438863.

[9] A. Dey, R. Guldiken and G. Mumcu, “Microfluidically reconfigured wideband frequency-tunable liquid-metal monopole antenna,” *IEEE Trans. Ant. Propag.*, **64**, 6, June 2016, pp. 2572-2576, doi: 10.1109/TAP.2016.2551358.

[10] N. C. Pradhan, M. G. Reddy, K. S. Subramanian, R. K. Barik, S. Koziel and Q. S. Cheng, “Microfluidic SIW-based tunable self-diplexing antenna for sub-6 GHz band applications,” *IEEE Trans. Circuits Syst. II: Exp. Briefs*, **70**, 4, April 2023, pp. 1435-1439, doi: 10.1109/TCSII.2022.3224234.